

# **Witness Sample Test Results for SQ-02 (LBNL), Practice Coils 1-3 (FNAL) and Practice Coils 2-4 (LBNL)**

E. Barzi, R. Bossert, D. Dietderich (LBNL), A. Ghosh (BNL), D. Turrioni

## Abstract:

The first step in the magnet R&D of the U.S. LHC Accelerator Research Program (LARP) is fabrication of technological quadrupoles TQS01 and TQC01. These are two-layer quadrupoles which use cables of same geometry made of 0.7 mm MJR Nb<sub>3</sub>Sn. From previous work [1], it was found that stability of this superconductor, as measured by the stability current,  $I_S$ , is very sensitive to the heat treatment schedule that is applied. The critical current,  $I_c$ , albeit less sensitive, also varies with the thermal cycle. To aid in the most appropriate choice of the heat treatment cycle of the actual TQ coils, the results obtained for the witness strand and cables samples used in the heat treatment of the SQ-02 and practice coil reactions are analyzed and summarized. Comparisons are made on measurements of  $I_c$  using the voltage-current (VI) method, of  $I_S$  as the minimal quench current obtained with the voltage-field (VH) method, and of RRR.

## **1. INTRODUCTION**

Modified Jelly Roll (MJR) with 54/61 filament design is being used for SQ-02, and both TQC01 [2] and TQS01 [3]. An important part of Nb<sub>3</sub>Sn magnet fabrication is the heat treatment, which is to be performed according to optimized schedules in vacuum or in an Argon atmosphere. Three heat treatments were so far performed. One for the SQ-02 coils at LBNL, one for TQ practice coils (PC) 1 & 3 at Fermilab, and another for TQ PC 2 & 4 at LBNL. In each case strand and cable samples were included in the retort together with the coils to serve as witnesses of the coil reaction. For this purpose it is important to know as accurately as possible both the thermal cycles seen by the coils and by the witnesses in term of temperatures and durations. These are usually not the same as the values set in the programmed cycles, due to thermal inertia and to the usually different location of the control thermocouples with respect to the coils. The witness samples are then tested for the critical current,  $I_c$ , using the voltage-current (VI) method, for  $I_S$  as the minimal quench current obtained with the voltage-field (VH) method, and for RRR. Short sample limit predictions for the coils can also be obtained.

## 2. STRAND AND CABLE WITNESS SAMPLES

### 2.1 Sample Description

Three billets by Oxford Superconducting Technology (OST) were used to fabricate the cables. The round strand properties as measured by OST are summarized in Table I, and the properties of the cables used as witness samples during the coil reactions are shown in Table II. This Table includes also a prototype cable, 933R, made of the most recent Restacked Rod Process (RRP) design with 54/61 filaments, as samples of this cable were included during practice coil reaction at LBNL.

For an accurate representation of the actual thermal cycles seen by the coils, thermocouples of type K were placed in various locations, as shown for instance in Fig. 1 in the case of the reaction of practice coils 1 and 3 at Fermilab. At LBNL each temperature was recorded by means of a paper chart at the rate of xxx. At Fermilab each temperature was recorded using a PC and LabView DAQ at the rate of 1 reading every 6 minutes. In both cases a temperature profile is obtained. Table III gives a representation of the thermal cycles using the average coil and witnesses temperatures and variations, and the crossing thresholds shown. Some considerations on threshold values can be found in the Discussion, Section 4.

TABLE I  
MJR STRAND PROPERTIES AS MEASURED BY OST

<b>Billet ID</b>	<b>Ore 205</b>	<b>Ore 206</b>	<b>Ore 208</b>
Cu %	46.7 ± 0.2	47.3 ± 0.3	47.4 ± 0.2
RH twist, mm	12	12	13
No. units	10	17	13
Total length, m	8517	8887	7514
Average length/unit, m	851	523	578
Standard deviation, m	697	445	345
I <sub>c</sub> (12 T) w/HT-1 <sup>a</sup> , A	423 ± 11	415 ± 1	439 ± 5
RRR w/HT-1 <sup>a</sup>	5	5	5
I <sub>c</sub> (12 T) w/HT-2 <sup>b</sup> , A	405 ± 10	384 ± 2	424 ± 4
RRR w/HT-2 <sup>b</sup>	21 ± 11	42 ± 6	42 ± 7

<sup>a</sup> HT-1 was 100 h at 210°C, 48 h at 340°C, 180 h at 650°C.

<sup>b</sup> HT-2 was 100 h at 210°C, 48 h at 340°C, 90 h at 650°C.

TABLE II  
WITNESS CABLES DESCRIPTION

<b>Cable ID</b>	<b>Nb<sub>3</sub>Sn technology</b>	<b>Strand No.</b>	<b>Pre-anneal dimensions, mm x mm</b>	<b>Pre-anneal angle</b>	<b>Re-roll dimensions, mm x mm</b>	<b>Re-roll Angle</b>	<b>Pitch, mm</b>
926R (SQ)	MJR	20	7.837 x 1.290	-	7.793 x 1.276	-	53.9*
928R-B (TQ)	MJR	27	10.054 x 1.304	1.019	10.052 x 1.266	1.062	78
932R-A (TQ)	MJR	27	10.039 x 1.304	0.968	10.053 x 1.262	1.026	78.5
933R (TQ)	RRP	27	10.035 x 1.304	0.928	10.042 x 1.267	1.078	77.5*

\* Set (as opposed to measured) pitch.

TABLE III  
THERMAL CYCLES DESCRIPTION

	SQ-02, LBNL			TQ P. Coils 1 & 3, FNAL			TQ P. Coils 2 & 4, LBNL		
	Time, h	Coil Ave. T, °C	Witness T, °C	Time <sup>a</sup> , h	Coil Ave. T, °C	Witness T, °C	Time, h	Coil Ave. T, °C	Witness T, °C
RT to 195°C	8.5			21 / 12.5			20		
195°C to 215°C	47	206.5 ± 1.5		42.5 / 50.5	210	213	37	206 ± 0.5	
215°C to 390°C	5			11.5 / 7.7			11		
390°C to 405°C	46	394.5 ± 1.5		38 / 42.5	400	401.5	40.5	395 ± 0.5	
405°C to 630°C	4			6.3 / 5			5.5		
630°C to 630°C	47.5	637.5 ± 1.5		44 / 45.3	645	645	45	638 ± 0.5	
640°C to 640°C	-	-	-	41 / 43	645	645	-	-	-
> 600°C	53			47.5 / 48.5			48		

<sup>a</sup> Time for coil / time for witnesses.

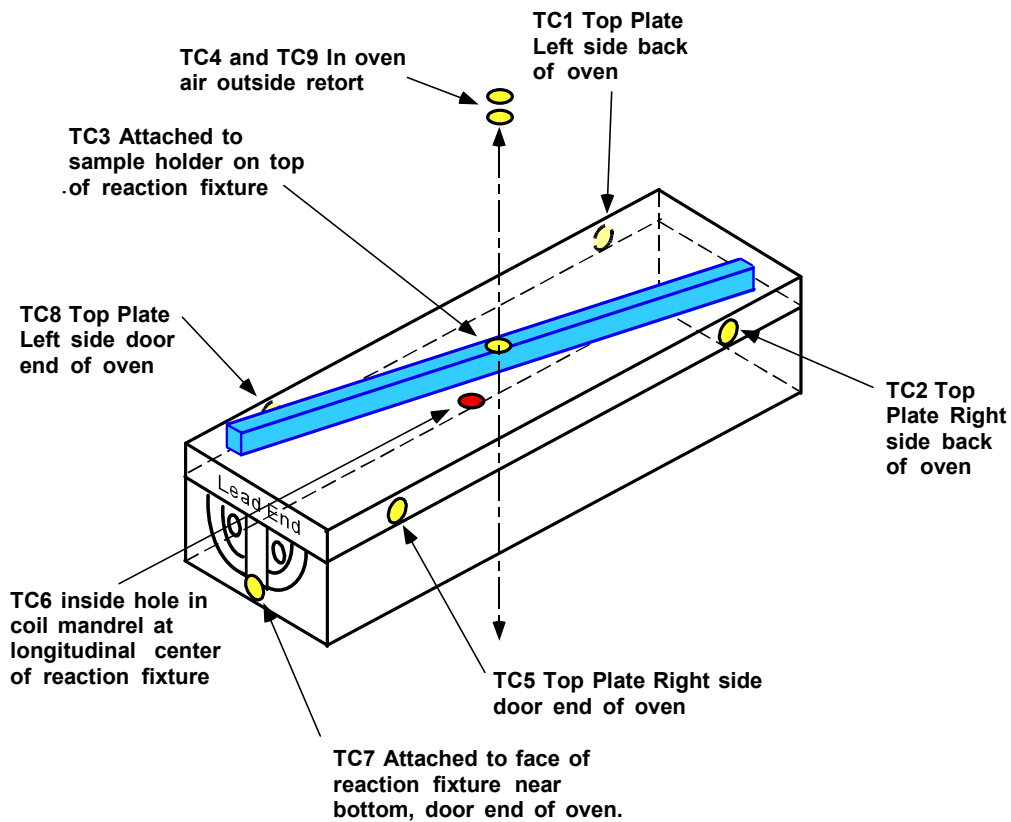


Fig. 1. Thermocouple locations during reaction of practice coils 1 & 3 at FNAL.

## 2.2 Sample List

The strand and cable samples used as witnesses in the three reactions are listed in Tables IV to VI.

TABLE IV  
WITNESS SAMPLES IN SQ-02 REACTION AT LBNL

TESTING LAB	STRANDS	CABLES
BNL	RD: 206-N, 208-F1. SQ extr.: 205-L	
FNAL	RD: 205-J, 206-N. SQ extr.: 206-F	926R (2x52 in)
LBNL	RD: 205-L, 208-F1. SQ extr.: 208-J	

TABLE V  
WITNESS SAMPLES IN PC-1&3 REACTION AT FNAL

TESTING LAB	STRANDS	CABLES
BNL	RD: 205-H, 206-F. TQ extr.: 205-M, 206-E2	
FNAL	RD: 205-G, 208-F1. TQ extr.: 205-M, 208-F2	928R-B (1x52 in)
LBNL	RD: 206-F, 208-F1. TQ extr.: 206-M2, 208-H2	

TABLE VI  
WITNESS SAMPLES IN PC-2&4 REACTION AT LBNL

TESTING LAB	STRANDS	CABLES
BNL	RD: 206-E2, 208-F2. TQ extr.: 206-E2, 208-F2	
FNAL	RD: 205-G, 206-F. TQ extr.: 205-G, 206-E1	928R-B (1x46in), 932R-A (1x46in), 933R (1x52in, 1x45in)
LBNL	RD: ?, ?. TQ extr.: ?, ?	

### 2.3 Test Procedures

The strand samples were mounted on grooved cylindrical barrels made of either Ti-6Al-4V (FNAL, LBNL) or stainless steel (BNL). After reaction, the samples were either tested on the same barrel (FNAL, LBNL) or transferred to a Ti-alloy barrel (BNL). Unless otherwise specified, strand samples are tested as follows:

- BNL uses end splices soldered in parallel to a couple of sample end turns and no stycast.
- FNAL uses no end splices and no stycast.
- LBNL uses end splices and stycast.

Tests were performed in He at 4.2 K, in a transverse magnetic field, with relative directions of external field and transport current such as to generate an inward Lorentz force. The voltage was measured along the sample by means of voltage taps placed 50 and 75 cm apart. In the case of smooth transition from the superconducting (SC) to normal state, the  $I_c$  was determined from the voltage-current (VI) curve using the  $10^{-14} \Omega\cdot m$  resistivity criterion. The  $I_c$  measurement uncertainty is typically within  $\pm 1\%$  at 4.2 K and 12 T. Voltage-field (VH) tests were performed by ramping to a fixed transport current, and sweeping the field up and down with ramp rates of 5 to 17 mT/s in the field ranges 0-4-0 T and 4-8-4 T. If no quench was observed the current was increased and the test repeated. This test was done to determine the minimum quench current, or stability current,  $I_s$ , in the presence of a magnetic field variation.

Cables quench currents were measured at self-field with a SC transformer equipped with a Rogowski coil to measure the secondary current. The  $Nb_3Sn$  cable sample is part of the secondary winding. The integrated Rogowski signal (proportional to the secondary current) and the primary current from the analog output of the power supply were acquired with a NI DAQ card at a 25 kHz rate.

### 3. RESULTS

Results of witness strand measurements are shown in Tables VII to IX, and those of witness cables in Table X. Their quench histories are shown in Figs. 2 and 3 in Appendix A.  $I_c$  values in between square parentheses were obtained using the parameterization in [4]. The  $I_S$  values in the Tables are the minimal actual quench currents observed. For the PC-24 witnesses, also FNAL used end splices. This extended the field range of stable VI curves down to 8 T in most cases. As can be seen, tests performed at FNAL on 0.7 mm extracted strands tested without stycast yield  $I_c$ 's that are lower than those obtained on similar samples at BNL, where samples are also tested without stycast. The little statistics presently available seems to indicate that stycast, by changing the strain conditions of the sample, may have an effect in increasing the  $I_c$  of extracted strands. Another parameter that may affect the results on extracted strands is the technique used in preparing the samples. In the meantime that this is better understood by making experiments and gathering more statistics, from FNAL tests only round strands should be considered for the purpose of analyzing the heat treatment effect on  $I_c$ .

TABLE VII  
SQ-02 WITNESS SAMPLE TEST RESULTS

Strand ID	$I_c$ , A at	15 T	14 T	13 T	12 T	11 T	10 T	8 T	$I_S$ , A	RRR	RRR <sup>b</sup>
205-J <sup>a</sup> , FNAL		166	224	292	371				1100	135	
206-N, FNAL		171	236	300	390		594	860	1200		188, 198?
Extr. 206-F, FNAL		damaged? (165 A at 12 T)									167
206-N, BNL					[389]	481	590	872	>1100	203	188, 198?
208-F1, BNL					[416]	511	626	914	>1200		172, 206?
Extr. 205-L, BNL		damaged? (295 A at 11 T)									128
205-L, LBNL											145
208-F1, LBNL											172, 206?
Extr. 208-J, LBNL				298	380	474	584		1200-1300		158

<sup>a</sup> Sample was transferred from LBNL barrel to FNAL barrel.

<sup>b</sup> Performed at LBNL using dedicated samples.

TABLE VIII  
PC-1&3 WITNESS SAMPLE TEST RESULTS

Strand ID	$I_c$ , A at	15 T	14 T	13 T	12 T	11 T	10 T	8 T	$I_S$ , A	RRR
205-G, FNAL		174	232	(307)	[387]				1000	80
Extr. 205-M, FNAL		142	187	240	304				1000	107
208-F1, FNAL		187	[250]	[324]	[412]				975	108
Extr. 208-F2, FNAL		144	192	248	313				1100	79
205-H, BNL					[445]	538	649	931	850	52
Extr. 205-M, BNL					[411]	502	610	881	1000	74
206-F, BNL					[436]	529	642	924	1050	88
Extr. 206-E2, BNL					[400]	489	600	874	1100	71

TABLE IX  
PC-2&4 WITNESS SAMPLE TEST RESULTS

Strand ID	$I_c$ , A at	15 T	14 T	13 T	12 T	11 T	10 T	8 T	$I_s$ , A	RRR
205-G, FNAL <sup>a</sup>		148	204	270	342		539	807	900	158
Extr. 205-G, FNAL <sup>a</sup>		149	200	263	333		513	(764)	1200	187
“ w/ stycast, FNAL <sup>a</sup>		172	232	301	380		(576)	(844)	1250	183
206-F, FNAL <sup>a</sup>		157	214	278	358		553		900	201
Extr. 206-E1 w/stycast, FNAL <sup>a</sup>		155	[207]	[272]	[350]				1100	158
206-E2, BNL		damaged?					366	454		>1200
Extr. 206-E2, BNL					[374]	461	569	836		> 1200
208-F2, BNL					[401]	492	602	879		1100
Extr. 208-F2, BNL					[401]	491	603	881		> 1200 193

<sup>a</sup> End splices were used.

TABLE X  
WITNESS CABLES TEST RESULTS

HEAT TREATMENT	Cable ID	Impregnation	Cable Ave. $I_q$ , A	Cable Min. $I_q$ , A	Ave. $I_q$ /strand, A	Min. $I_q$ /strand, A
SQ-02 at LBNL	926R (SQ)	Y	18362	17965	918	898
“	“	N	18874	17846	943	892
PC-1&3 at FNAL	928R-B (TQ)	Y	19836	18827	734	697
“	“	N	19706	18593	729	688
PC-2&4 at LBNL	928R-B (TQ)	N	20391	19773	755	732
“	932R-A (TQ)	N	23472	22981	869	851
“	933R (TQ)	N	22581	20569	836	762
“	“	N	20114	15740	745	583

## 4. DISCUSSION

Heat treatment (HT) optimization includes:

- Improve high field  $I_c$ , which depends on the last step of the HT.
- Improve low field  $I_s$ , which also depends on the last step of the HT.
- Avoid Sn leaks, which depend on the low steps of the HT.

The following is also discussed:

- Crossing thresholds in thermal cycles.
- Are witness samples good predictors of magnet performance?

### High field $I_c$

Was highest for PC-13 HT, with 41 h (43 h for witnesses) at 645°C.

Was lowest for PC-24 HT, with 45h at 638°C.

If there is a measurable difference in  $I_c$  between SQ-02 HT, with 47.5 h at 637.5°C, and PC-24 HT, it means that at ~638°C  $I_c$  is still on the rise after 45 h. If this were true it would mean that a temperature of 638°C would require an excellent control on duration.

## Low field $I_s$

Was highest in SQ-02 HT, was similar in PC-13 and PC-24, a little larger in PC-24. This is found in both strand and cable tests, which typically yield ~150-200 A less per strand than the strand test. Little difference was so far seen between impregnated and non-impregnated cable samples.

However, the RRR resulting from PC-13 are about half of those resulting from PC-24.

## Sn leaks

The PC-24 HT, with 37 h at 206°C, produced Sn leaks in practice coil No. 2, whereas SQ-02 HT, with 47 h at 206.5°C, and PC-13 HT, with 42.5 h at 210°C, did not produce any Sn leaks. These Sn leaks were produced extensively enough in practice coil 2 (two locations in the outer layer and two in the inner layer, not including lead ends) to exclude localized damage in the strands. A problem with cable quality should presumably also be excluded since practice coils 1, 2 and 3 were made out of the same cable. All of the above prompts to address attention to the HT. All coils were made of a hot extruded strand instead of MJR. Whereas no Sn leaks were observed in the MJR cable samples used as witnesses, since Sn leaks have been observed in the past in coils made of similar MJR strands, this Sn leak problem cannot be ignored.

During solid Cu-Sn diffusion at 210°C, layers of eta and epsilon Cu-Sn intermetallic phases form around the Sn rods, as shown in Fig. 10 in Appendix B [5]. When the material is brought up to the second temperature step (typically between 340°C and 400°C), it crosses the liquefaction point of Sn at 227°C. It is important that when the Sn liquefies, the surrounding shells be thick enough to hold its hydrostatic pressure. Estimating how thick were the shells between 37 and 47 h at ~206°C would provide a lower limit to their desirable thickness. Figs. 4 to 7 in Appendix B show the thickness of eta and epsilon phases that formed with time in Cu-Sn models (Fig. 12) that provided an infinite (i.e. non-depletable) supply of Sn. Since in the strands the Sn undergoes a depletion process, the intermetallic thickness measured in the models ends up being larger in time than what is measured in strands, and should be therefore taken as an upper limit of what happens in strands of any Sn content. This can be seen for instance in Figs. 8 and 9, where the thickness measurements on models are compared with those found in ITER strands at 210°C and at 400°C. From Fig. 8 it appears that at 210°C between 24 h and 72 h the eta and epsilon intermetallic layers in the strand are still growing from ~3 μm or less up to ~4 μm, within the measurement uncertainties. The minimum acceptable intermetallic thickness seems therefore to be somewhere in between. Figs. 11 and 12 show magnified subelements of the ITER and MJR strands with their size scales. One can see that the size of the Sn rod in the MJR is very similar, maybe only a little smaller than that of the ITER, which was measured to be ~50 μm. In summary, it is possible that an extra thickness of the order of the micrometer is what makes the shells strong enough. Hence it makes sense to spend at least 3 days (72 h) at 210°C to allow the intermetallic eta and epsilon shells to grow each by an extra micrometer or so. It would require four more days at 210°C to add another micrometer.

## Crossing thresholds in thermal cycles

The plots in Figs. 4 to 7 can be used to infer an approximate sensitivity of intermetallic thickness to temperature for a given duration. Since in the vicinity of 210°C the epsilon phase obtained in the Cu-Sn models follows best the behavior in the strand, the plots on epsilon formation in Figs. 5 and 7 were used to obtain (with linear interpolation) a  $dT/d\_thickness$  of ~27°C/μm in the vicinity of 210°C for durations of ~72 h. This increases to ~35°C/μm for durations of 24 h, which is about the time it took for PC-13 to go from 195°C to 210°C. Using 195°C and 215°C as thresholds for the 210°C step is

hence likely to produce uncertainties of about  $\pm^{0.2}_{0.5}$   $\mu\text{m}$  on the eta and epsilon thicknesses. Temperature thresholds of 205°C and 215°C would improve the uncertainties to  $\pm 0.2$   $\mu\text{m}$ . It is also important that the temperature in this step never crosses the liquefaction point of Sn, which is 227°C for the Cu-Sn system.

At 400°C Sn depletion in the strand occurs very fast (in less than 10 h) and in less than a day (Fig. 9) the epsilon phase has reached the maximum thickness allowed by the Cu-Sn composition in the strand, as shown in Fig. 10 (right). From that point on nothing changes anymore. By using the same method as in the previous case, temperature thresholds of 380°C and 420°C should be adequate for a duration of 48 h.

An average  $dI_c/dT$  that was found for the MJR strand at 11 T is  $\sim 1.6$  A/°C, with  $I_c$ 's(11 T) in the 457 A to 537 A range. Temperature uncertainties (with respect to  $T_{\text{nominal}}$ ) of  $\pm 5^\circ\text{C}$  would produce an uncertainty on the  $I_c$  of  $\sim \pm 2\%$  or less.

## Use of witnesses as predictors of coil performance

Ideally witnesses should be able to predict both high field and low field (i.e. stability) performance.

A comparison available so far between witness predictions and coil test results is that of the SQ-02. Already as it is, with the witness predicting only 2 to 3% more of actual coil performance, there is a very good consistency. Moreover, in this prediction three effects were not considered. A temperature effect due to the coil being tested at 4.3 K (samples are tested at 4.2 K), which would reduce the high field  $I_c$  of  $\sim 1\%$ . A billet blend effect due to the short sample limit being calculated for the best performing billet, Ore 208, which would reduce the high field  $I_c$  of  $\sim 4\%$ . A strain effect due to the samples being tested on Ti-alloy barrels, which put the samples under tensile strain thereby increasing their inherent  $I_c$ . These reductions have to be applied against the coil load line to obtain the appropriate reduction on the coil current.

When heat treating coils with larger thermal masses, it makes sense to monitor the witnesses with dedicated thermocouples. This was done for instance for PC-13, where in Table III temperatures and durations associated to the witnesses samples are also shown. As can be seen, the last step (which determines  $I_c$  and  $I_S$ ) temperature is the same as for the coils, and the duration only slightly different. In general witness samples appear to have shorter ramp rates, and therefore longer dwell times.

Low field performance is measured on both strands and cables. Cables at self-field appear to quench at currents that are systematically lower than in strands. The prediction on magnet stability performance improves with test statistics. However, if the superconductor is subject to filament merging, like in some RRP materials, which is a local effect, predictions made on cables can be as much as 100% off with respect to the magnet.

## REFERENCES

- [1] E. Barzi et al., “Round and Extracted Strand Tests for LARP Magnet R&D”, paper TUA2OR5, MT-19.
- [2] R. Bossert et al., “Development of a 90-mm  $\text{Nb}_3\text{Sn}$  Technological Quadrupole for LHC Upgrade based on SS Collar”, paper WEA07PO08, MT-19.
- [3] S. Caspi et al., “Design and construction of TQS01 - a 90-mm  $\text{Nb}_3\text{Sn}$  quadrupole model for LHC luminosity upgrade based on a key and bladder structure”, paper WEA07PO03, MT-19.
- [4] L. T. Summers et al., “A model for the prediction of  $\text{Nb}_3\text{Sn}$  critical current as a function of field, temperature, strain and radiation damage”, IEEE Trans. Magn., 27 (2): 2041-2044, 1991.
- [5] Sara Mattafirri's Laurea Thesis.

# APPENDIX A

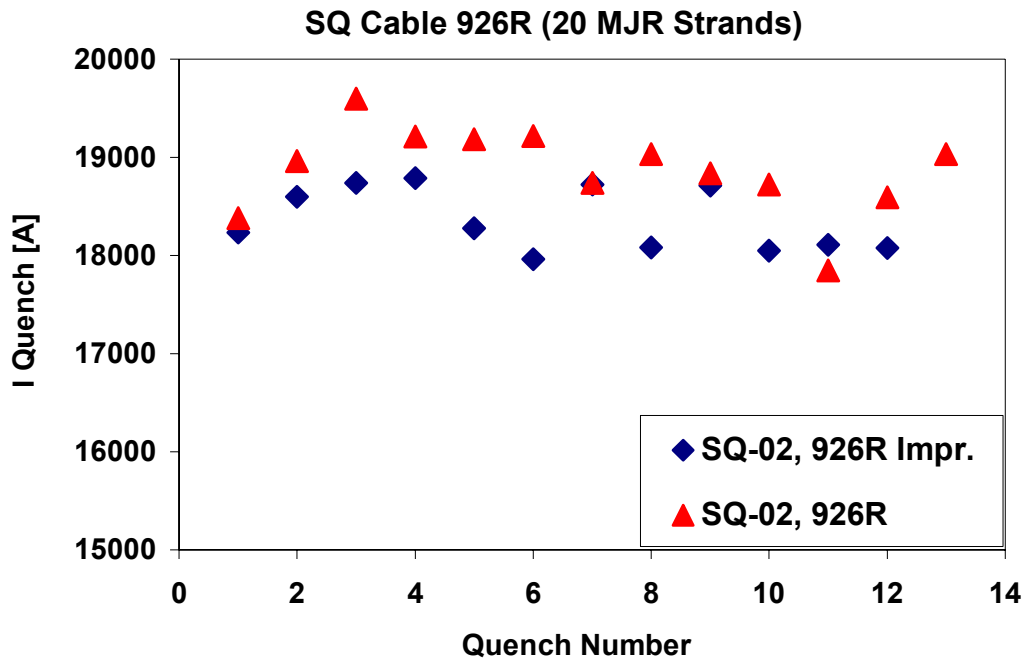


Fig. 2. Quench histories of cable samples 926R used as witnesses of SQ-02 reaction.

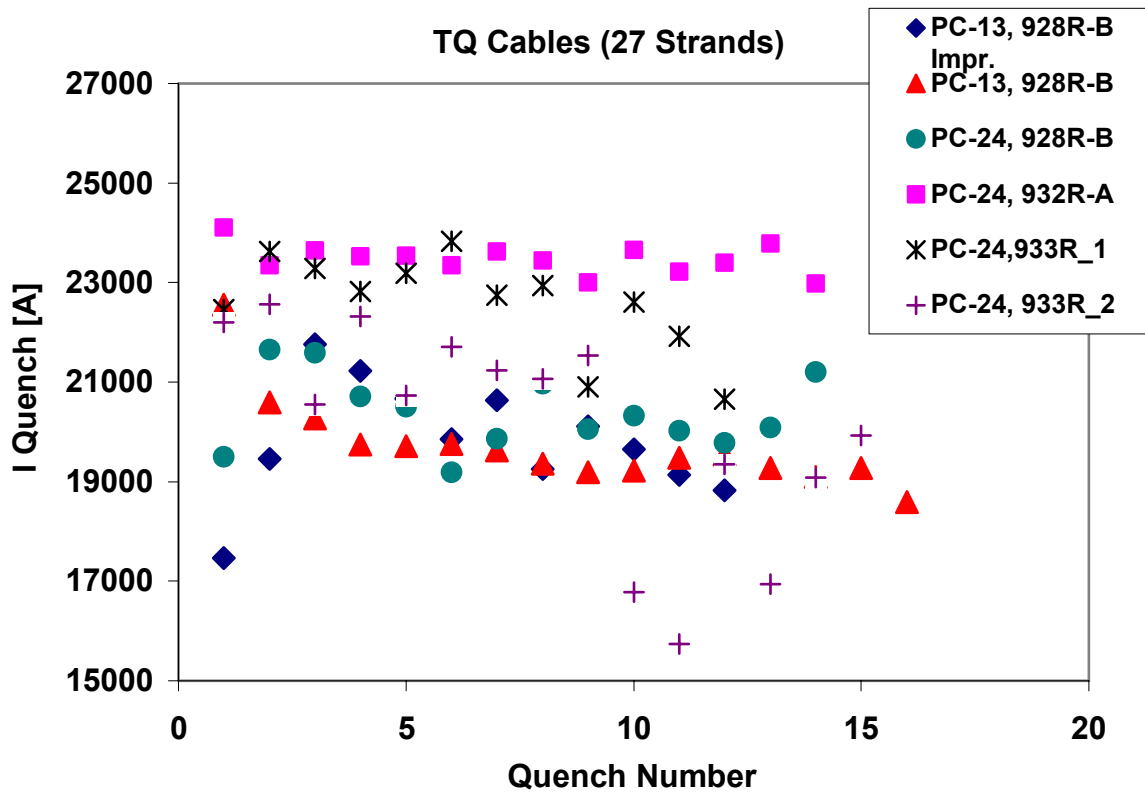


Fig. 3. Quench histories of TQ cable samples used as witnesses of PC-13 and PC-24 reactions.

APPENDIX B (from ref. [5])

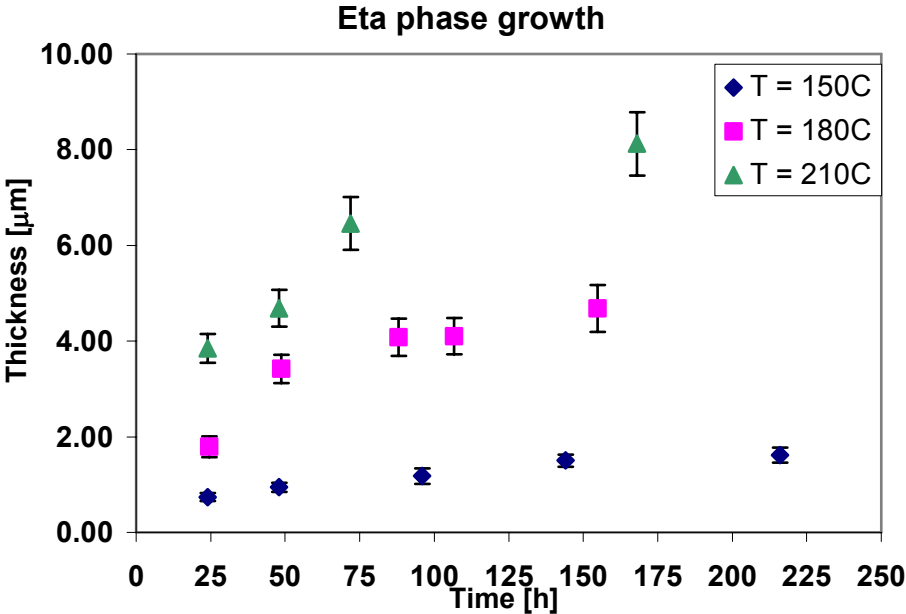


Fig. 4. Thickness of eta phase forming with time in Cu-Sn models up to 210°C.

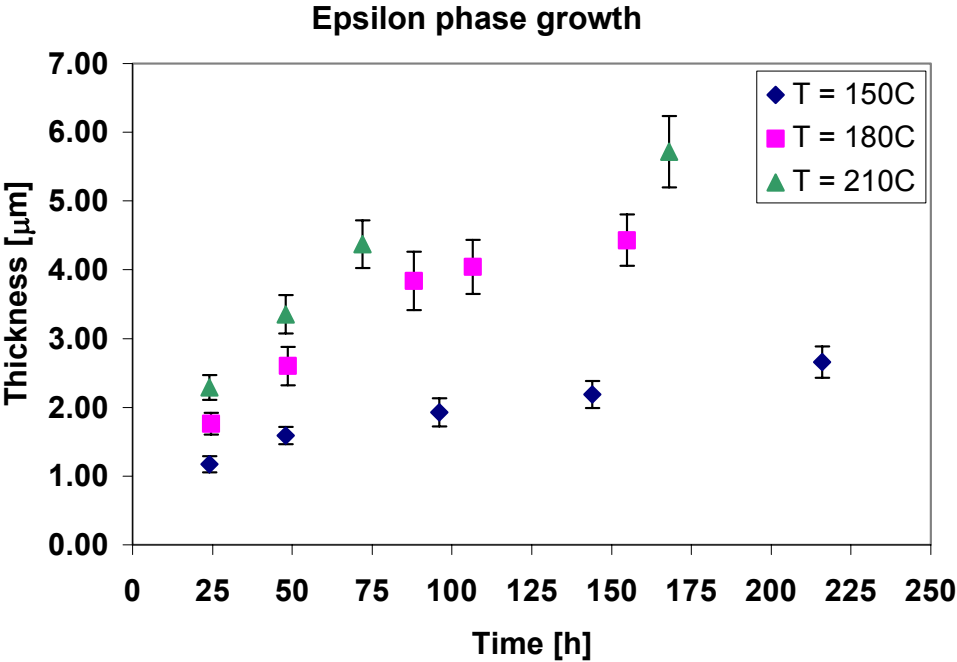


Fig. 5. Thickness of epsilon phase forming with time in Cu-Sn models up to 210°C.

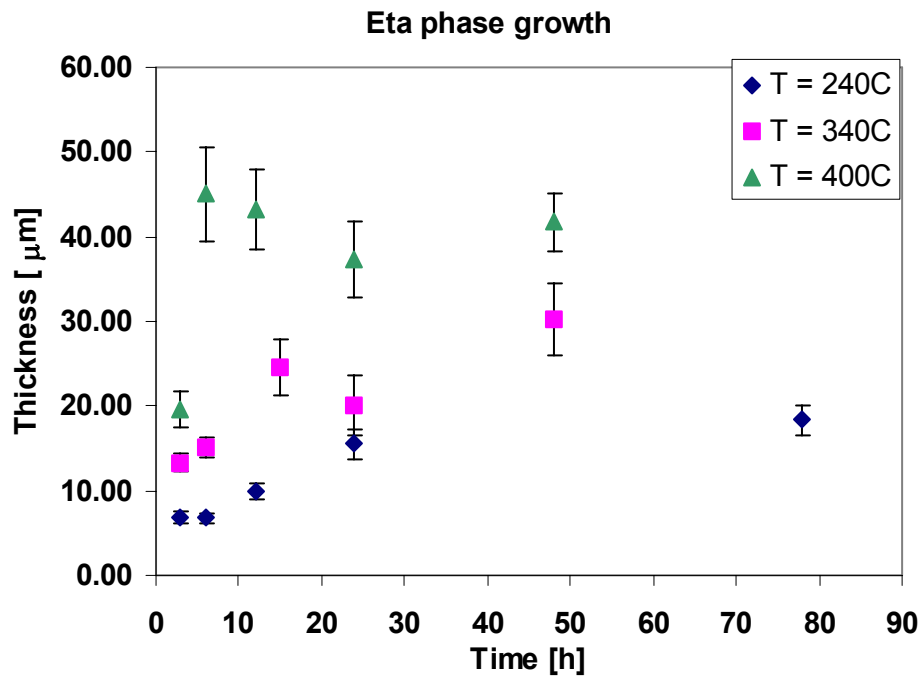


Fig. 6. Thickness of eta phase forming with time in Cu-Sn models above 210°C.

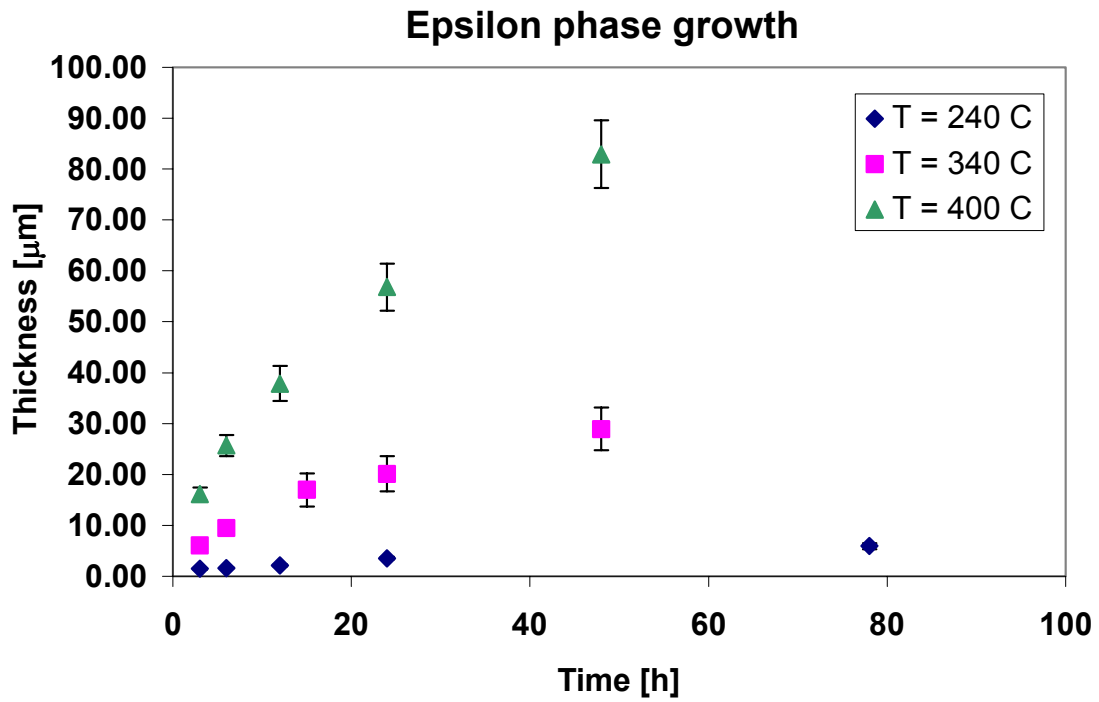
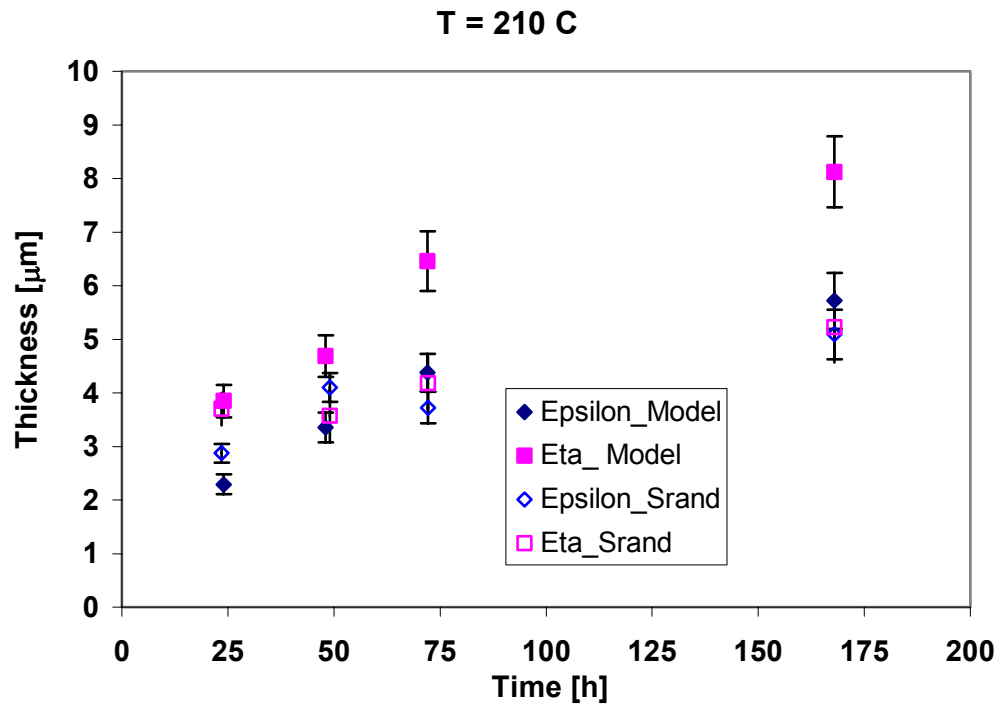
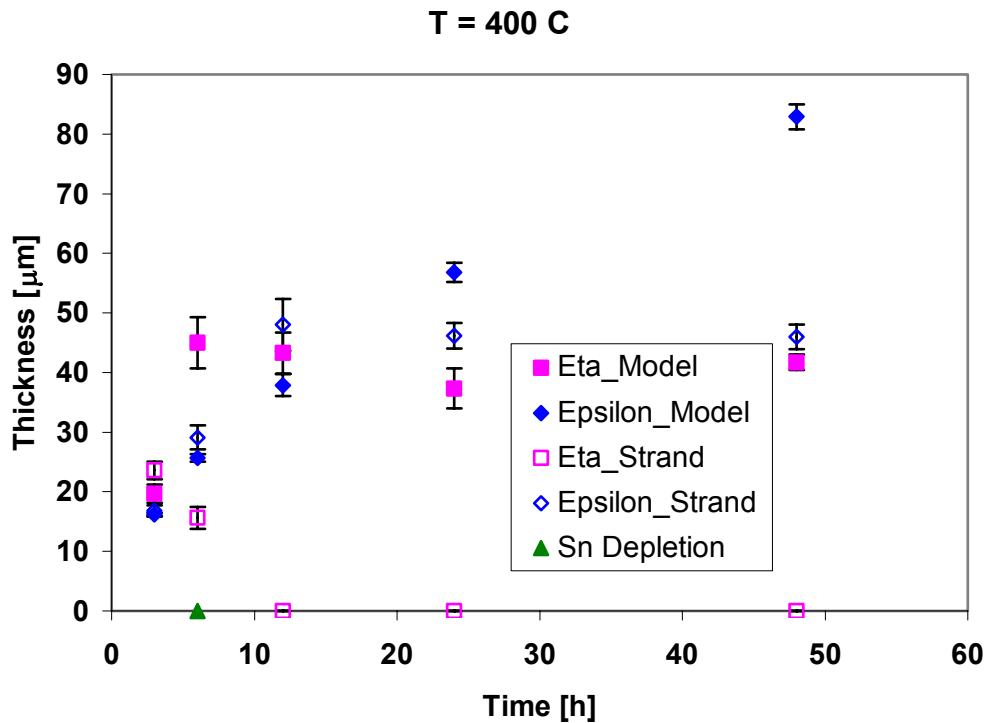


Fig. 7. Thickness of epsilon phase forming with time in Cu-Sn models above 210°C.



**Fig. 8.** Thickness comparison of eta and epsilon phase forming at 210°C between the Cu-Sn model and the ITER strand.



**Fig. 9.** Thickness comparison of eta and epsilon phase forming at 400°C between the Cu-Sn model and the ITER strand.

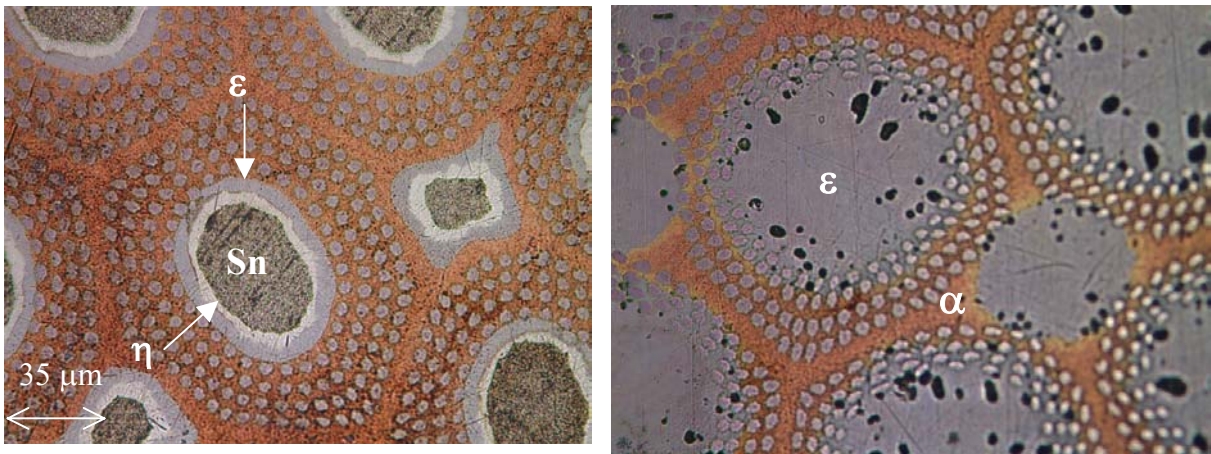


**Fig. 10.** ITER strand cross section after one week at 210°C (left) and after 48 h at 400°C (right).

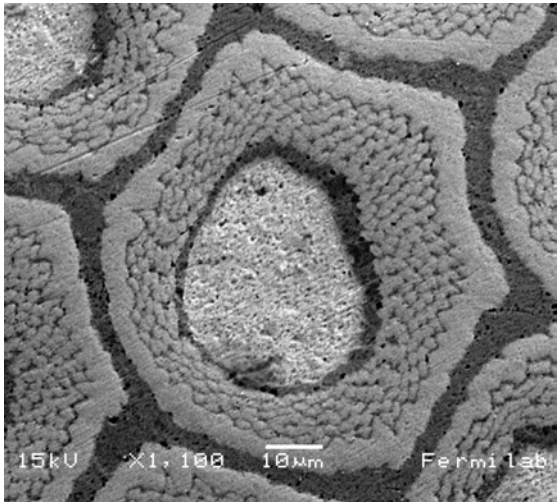


**Fig. 11.** SEM of MJR subelement before reaction.

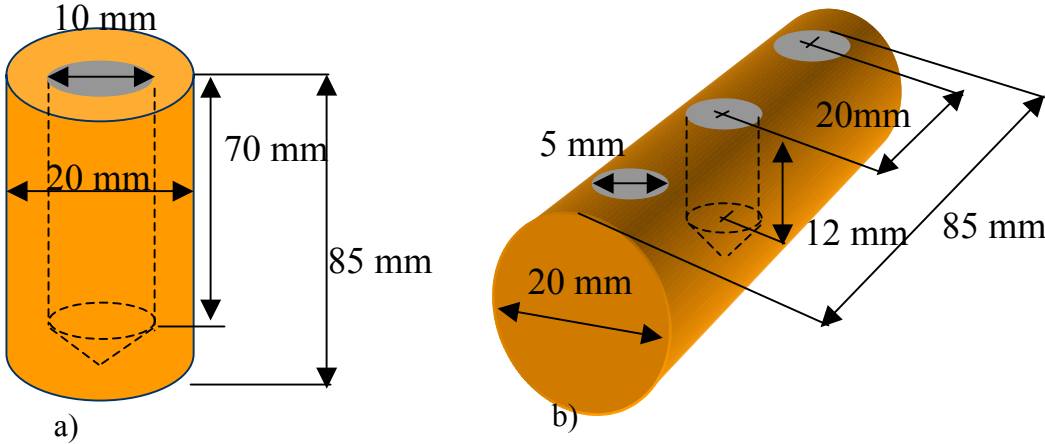


**Fig. 12.** Cu-Sn model used up to 210°C (left) and above 210°C (right).